On the Characterization of Foam Decay with Diagram Lattices and Majorization

Sonja Sauerbrei, Uwe Sydow, and Peter J. Plath

Institut für Angewandte und Physikalische Chemie – AG Chemische Synergetik, Universität Bremen, Bibliothekstraße NW2, D-28359 Bremen, Germany

Reprint requests to Prof. P.J. P.; E-mail: plath@uni-bremen.de

Z. Naturforsch. **61a,** 153 – 165 (2006); received November 14, 2005

We present possibilities of comparing and characterizing bubble size distributions during foam decay. We know that the temporal development of bubble size distributions does not follow an ordinary diffusion process. Instead of an equal distribution, we obtain a multi-modal distribution at the end of the rearrangement phase. It turns out that bubble size distributions are comparable to partition diagrams generating Ruch lattices which are expandable by permutations leading to partially ordered sets. If we map the partition diagrams and the bubble size distributions on the Shannon entropy, we obtain similar functions. Furthermore, the set of partition diagrams of a Ruch lattice and the set of the bubble size distributions of foam decay are both partially ordered. Via the theorems of Muirhead and of Hardy, Littlewood and Pólya (classical majorization) we construct transitions between every partition diagram of a Ruch lattice and between every bubble size distribution. These transitions can be reversible or irreversible.

Key words: Foam Decay; Bubble Size Distribution; Majorization; Diagram Lattices.

1. Introduction

Inspired by our first publication on beer foam [1], we continued to study the fascinating system foam. Motivated by the work of E. Ruch [2], we represented partition diagrams as vectors (Fig. 9) which are comparable via partial sums (Fig. 10). E. Ruch established a "greater relation" among partition diagrams through the comparison of partial sums. He said a partition diagram as a vector $\boldsymbol{\gamma'}$ has a greater mixing character than a partition diagram as a vector $\boldsymbol{\gamma}$, if

$$\sum_{i=1}^{k} \gamma_i^* \geq \sum_{i=1}^{k} \gamma_i'^*; k = 1, 2, \cdots, n-1, \text{and} \qquad (1)$$

$$\sum_{i=1}^{n} \gamma_i = \sum_{i=1}^{n} \gamma_i'. \qquad (2)$$

$\boldsymbol{\gamma}^* = (\gamma_1^*, \gamma_2^*, \cdots, \gamma_n^*)$ denotes the n-tuple rearranged in nonincreasing order, $\gamma_1^* \geq \gamma_2^*, \geq \cdots \geq \gamma_n^*$ (Ruch used the notation $\boldsymbol{\gamma}$ and $\boldsymbol{\gamma'}$, but we will compare $\boldsymbol{\alpha}$ and $\boldsymbol{\beta}$ with each other). If two vectors do not satisfy (1), they are called incomparable. (2) describes the trace of the vectors (the sum of the vector components is the trace). Through this "greater relation" E. Ruch generated a lattice of the partition diagrams of an integer and obtained partially ordered lattices for integers ≥ 6 (Fig. 8). We will call these partially ordered lattices Ruch lattices.

Uhlmann [3] compared two vectors by saying $\boldsymbol{\beta}$ is more mixed than $\boldsymbol{\alpha}$ if there exists a doubly stochastic matrix $\mathbf{S}$ satisfying $\mathbf{S}\boldsymbol{\alpha} = \boldsymbol{\beta}$ [provided both vectors have nonnegative integers and the same trace (2)]. These doubly stochastic matrices can be generated by the theorems of Muirhead [4] and of Hardy, Littlewood and Pólya [5].

Now every Ruch lattice of an integer consists of a specific number of partition diagrams [6]. As the vectors of partition diagrams of an integer n should be n-dimensional, they are expanded with zero elements. The vector elements can be permuted, and we obtain a specific number $P(n)$ of permutations of this vector. Then the sum of all vector permutations is a specific number of permutations of a Ruch lattice.

That way we see many possibilities to apply this Ruch model to our bubble size distributions. Now we want to test this mathematical approach for the foam system. But first we consider the characteristics of this system again.

2. Foam – A System with Unusual Behaviour

How does foam decay? It is our intention to go further into this question. We used beer foam because it is

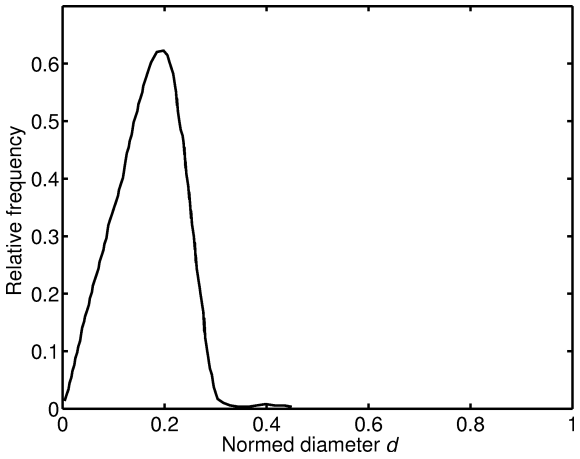

Fig. 1. The narrow bubble size distribution 30 s after being frothed up with ultrasound.

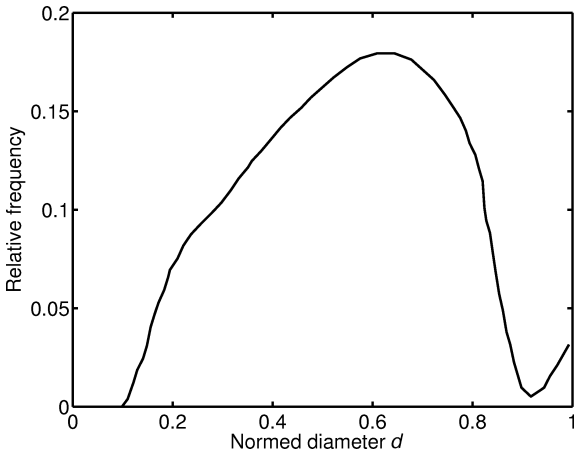

Fig. 2. The broad mono-modal bubble size distribution after 60 s as a result of the processes in the foam.

of special interest in the brewing industry for the quality management of beer, and the time scale of the decay is manageable. To create defined initial conditions, the beer is frothed up with ultrasound in a measuring glas (see Section 7). Because of the frothing up with ultrasound, we obtain a narrow bubble size distribution [1, 7] (see Fig. 1). The histograms of the bubble size distribution are acquired as follows: The bubble sizes (bubble diameter d [μm]) are divided into ten size intervals: $(0 < d < 50 : 0.1;\ 50 < d < 100 : 0.2;\ 100 < d < 150 : 0.3; \cdots\ 400 < d < 450 : 0.9;\ 450 < d < 500 : 1)$. The ratio of the number of bubbles within an interval to the total number of bubbles at time t [s] represents the relative frequency.

After a few seconds the bubble size distribution becomes broader, e. g. other bubble sizes are created as a result of processes in the foam like gas exchange between the bubbles, collapsing and merging of bubbles. As can be seen in Fig. 2, almost all bubble size intervals are represented in a more or less broad mono-modal distribution.

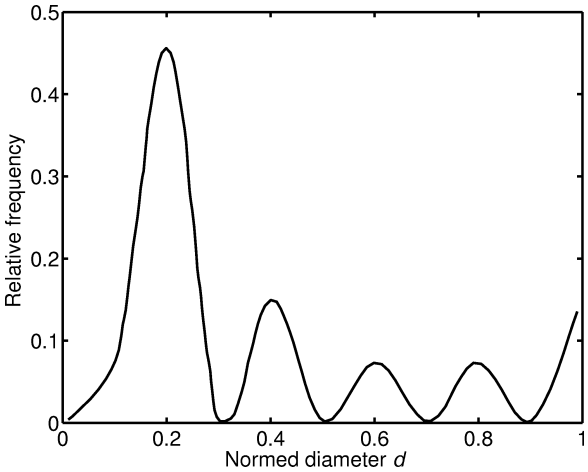

Fig. 3. The multi-modal bubble size distribution after 260 s at the end of the rearrangement in the foam [1].

After almost complete drainage of the foam, rearrangement and gas exchange processes become dominant. At the end of the rearrangement [1], the bubble size distribution develops into a multi-modal distribution with narrow peaks. This multi-modal distribution can be seen in Figure 3.

Between the broad mono-modal distribution (after 60 s) and the multi-modal distribution (after 260 s), the bubble size distribution splits up and drifts. In Figure 4 we see the maximum of the bubble size interval at 0.6 units split up in two maxima at the bubble size intervals 0.4 and 0.9, respectively. 100 s later (Fig. 5) one maximum is at the bubble size interval 0.2, and the other maximum is the bubble size interval 1. After further 75 s the multi-modal distribution is fully developped with maxima at 0.2, 0.4, 0.6, 0.8, and 1, see Figure 5.

Now we consider the temporal development of several bubble size intervals. The ratio of the number of bubbles within a bubble size interval at a certain time to the number of all bubbles within this bubble size interval at all times against the time is plotted to compare several bubble size intervals. We find a damped oscillating behaviour (Figs. 6 and 7). Furthermore, there are bubble size intervals developing approximately parallel. We like to call this behaviour “in-phase” (Fig. 6), and there are bubble size intervals developing contrarywise which we like to call “out-of-phase” (Fig. 7).

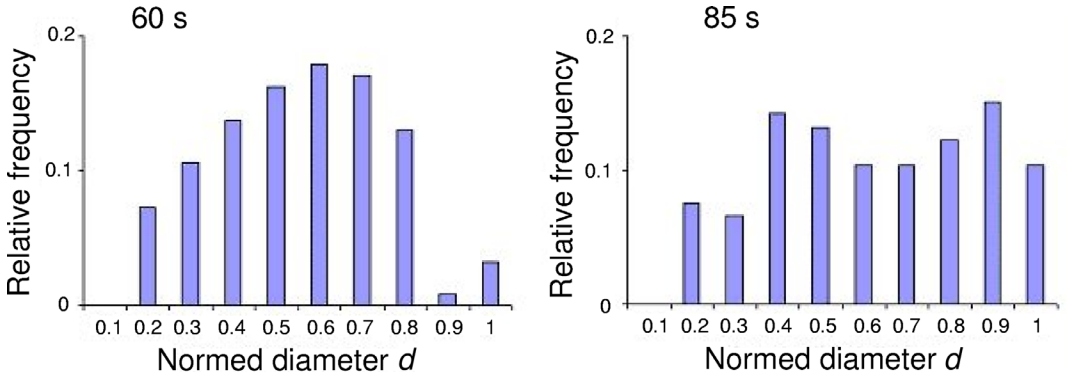

Fig. 4. The mono-modal bubble size distribution after 60 s splits up into two maxima at the bubble size intervals 0.4 and 0.9 25 s later.

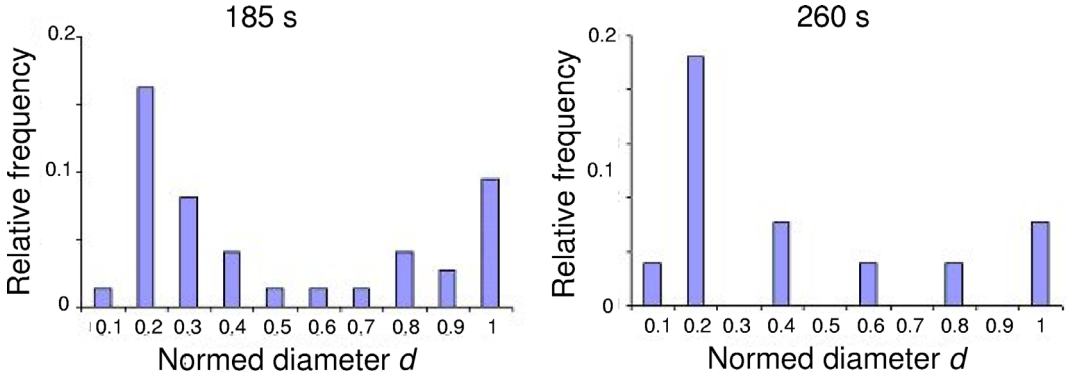

Fig. 5. After 185 s the two maxima are at the bubble size intervals 0.2 and 1. We obtain the multi-modal bubble size distribution after 260 s.

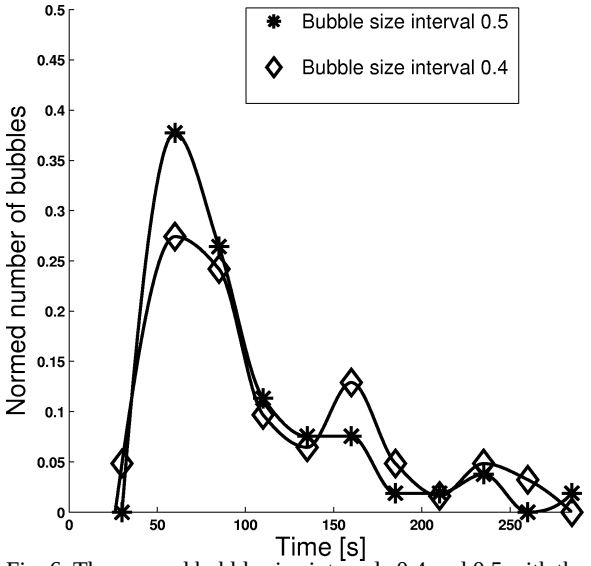

Fig. 6. The normed bubble size intervals 0.4 and 0.5 with the in-phase behaviour.

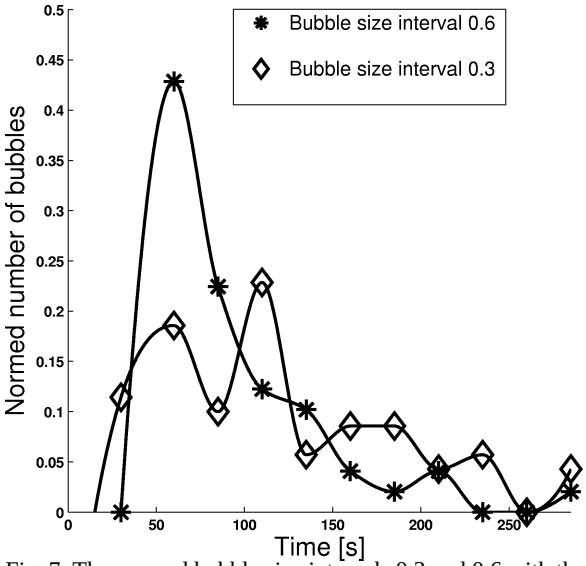

Fig. 7. The normed bubble size intervals 0.3 and 0.6 with the out-of-phase behaviour.

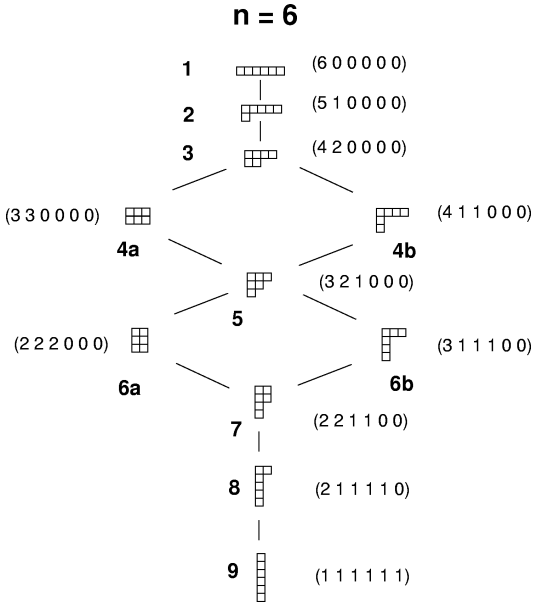

Fig. 8. Partially ordered $n = 6$ lattice according to Ruch [2] with corresponding state vectors.

3. Doubly Stochastic Matrices

It is easy to see that the $n = 6$ lattice in Fig. 8 consists of the partitions of the number 6. Thus the diagrams are called partition diagrams. Now we can understand such a partition diagram of a Ruch lattice as a histogram or in other words a finite discrete distribution, i.e. a partition diagram is comparable to an intrasystem state (the foam system). To characterize the progression of the partition diagrams (the progression describes a diffusion process with incomparable states) from the least upper bound to the greatest lower bound we map the partition diagrams (and intrasystem states, respectively) on vectors (state vectors). Later we like to characterize the temporal development of the bubble size distributions which will be mapped on vectors too. The vectors in Fig. 8 are 6-dimensional because we consider the partitions of the integer $n = 6$. As already mentioned, the vectors are expanded with zero elements. In Fig. 9 we watch as a partition becomes an n-dimensional vector for $n = 6$.

Such a partition diagram and state, respectively, consists of the integers of the partition. We can understand these integers as components of a vector and obtain state vectors, such as in Figure 9.

If we compare these vectors (state vectors) with each other, we will say vector $\boldsymbol{\alpha}$ is more mixed than vector $\boldsymbol{\beta}$, if there is a doubly stochastic transformation $\mathbf{S}$ satisfying

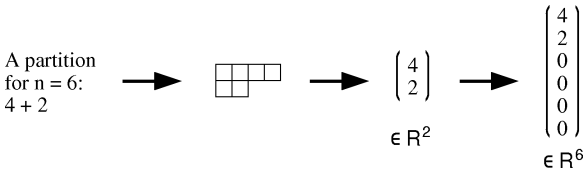

Fig. 9. The partition $4+2=6$, represented as a partition diagram of the $n = 6$ Ruch lattice. A partition diagram is comparable to a histogram or an intrasystem state. The integers of the partition can be mapped on a 2-dimensional vector. To obtain vectors with the same dimension within a Ruch lattice we expand the 2-dimensional vector with zero elements. These vectors are comparable to state vectors. The lowest common dimension of all partition vectors of the integer 6 is 6.

$$\boldsymbol{\alpha} = \mathbf{S}\boldsymbol{\beta}. \tag{3}$$

$\mathbf{S}$ is doubly stochastic. (We further mention other ways to express "$\boldsymbol{\alpha}$ is more mixed than $\boldsymbol{\beta}$" by saying "$\boldsymbol{\alpha}$ is more chaotic than $\boldsymbol{\beta}$", or by stating "$\boldsymbol{\alpha}$ is less pure than $\boldsymbol{\beta}$" (Thirring). Ruch, Mead and Schlögl say "$\boldsymbol{\alpha}$ has greater mixing character than $\boldsymbol{\beta}$" or even "$\boldsymbol{\alpha}$ is of larger mixing distance as compared with $\boldsymbol{\beta}$" [3].)

Doubly stochasticity of $\mathbf{S}$ firstly means $\mathbf{S}\boldsymbol{\beta} \geq 0$ if only $\boldsymbol{\beta} \geq 0$ ("positivity preserving"), and secondly $\mathrm{Tr}(\mathbf{S}\boldsymbol{\alpha}) = \mathrm{Tr}(\boldsymbol{\alpha})$ holds for all $\boldsymbol{\alpha}$ ("trace preserving", that means the sum of the vector components has the same value) [3].

The state vectors have to fulfil the condition that they are real nonnegative n-tuples which have the same trace. A doubly stochastic matrix is a matrix $\mathbf{S} = \alpha_{ij}$ such that

$$\alpha_{ij} \geq 0 \qquad \text{and} \qquad \sum_i \alpha_{ij} = \sum_j \alpha_{ij} = 1. \tag{4}$$

In other words, a nonnegative matrix is called doubly stochastic if all its row and column sums are one. Clearly, a doubly stochastic matrix must be square [8].

Now we will specify the conditions, and we want to show how to obtain a doubly stochastic matrix. Since an understanding of the classical concept of majorization is essential for our work, we will cite in detail the theorems of Muirhead [4] and of Hardy, Littlewood and Pólya [5, 8] in the following section.

4. Theorems of Muirhead and of Hardy, Littlewood and Pólya

"We introduce the following notation. If $\boldsymbol{\gamma} = (\gamma_1, \gamma_2, \cdots, \gamma_n)$ is a real n-tuple, then $\boldsymbol{\gamma}^* = (\gamma_1^*, \gamma_2^*, \cdots, \gamma_n^*)$

denotes the n-tuple $\boldsymbol{\gamma}$ rearranged in nonincreasing order, $\gamma_1^* \geq \gamma_2^* \geq \cdots \gamma_n^*$.

Definition 1. A nonnegative n-tuple $\boldsymbol{\alpha} = (\alpha_1, \alpha_2, \cdots, \alpha_n)$ is said to be majorized by a nonnegative n-tuple $\boldsymbol{\beta} = (\beta_1, \beta_2, \cdots, \beta_n)$

$$\alpha_1^* + \alpha_2^* + \cdots + \alpha_k^* \leq \beta_1^* + \beta_2^* + \cdots + \beta_k^*, \quad (5)$$

for $k = 1, 2, \cdots, n-1$, and

$$\alpha_1 + \alpha_2 + \cdots + \alpha_n = \beta_1 + \beta_2 + \cdots + \beta_n. \quad (6)$$

This is denoted by $\boldsymbol{\alpha} \prec \boldsymbol{\beta}$.

Let $\boldsymbol{\alpha}$ and $\boldsymbol{\beta}$ be real nonnegative n-tuples. Then $\boldsymbol{\alpha} \prec \boldsymbol{\beta}$ if and only if there exists a doubly stochastic $n \times n$ matrix $\mathbf{S}$ such that

$$\boldsymbol{\alpha} = \mathbf{S}\boldsymbol{\beta}. \quad (7)$$

Now we want to show that there exists a doubly stochastic matrix such that $\boldsymbol{\alpha} = \mathbf{S}\boldsymbol{\beta}$. Clearly, it is sufficient to prove that $\boldsymbol{\alpha}^* = \mathbf{S}\boldsymbol{\beta}^*$. If $\boldsymbol{\alpha}^* = \mathbf{P}\boldsymbol{\alpha}$ and $\boldsymbol{\beta}^* = \mathbf{Q}\boldsymbol{\beta}$, where $\mathbf{P}$ and $\mathbf{Q}$ are permutation matrices, then $\boldsymbol{\alpha} = (\mathbf{P}^T\mathbf{S}\mathbf{Q})\boldsymbol{\beta}$. We can assume therefore that $\boldsymbol{\alpha} = \boldsymbol{\alpha}^*$ and $\boldsymbol{\beta} = \boldsymbol{\beta}^*$. Suppose that $\alpha^* \neq \boldsymbol{\beta}^*$. Call the number of nonzero coordinates in $\boldsymbol{\beta}^* - \alpha^*$ the *discrepancy* between $\boldsymbol{\alpha}$ and $\boldsymbol{\beta}$, and denote it by $\delta(\boldsymbol{\alpha}, \boldsymbol{\beta})$. Since $\alpha^* \neq \boldsymbol{\beta}^*$, it is clear that $\delta(\boldsymbol{\alpha}, \boldsymbol{\beta}) \geq 2$. Since $\sum_{i=1}^{n}(\alpha_i - \beta_i) = 0$ and not all these differences can be zero, some of them must be positive and some negative. Let t be the least subscript such that $\alpha_t > \beta_t$, and let s be the greatest subscript, less than t, for which $\alpha_s < \beta_s$."

For example, let $\boldsymbol{\alpha} = (9\ 6\ 5\ 4\ 4)$ and $\boldsymbol{\beta} = (10\ 10\ 5\ 2\ 1)$. Then $\boldsymbol{\alpha} \prec \boldsymbol{\beta}$ (Definition 1). Find a doubly stochastic matrix $\mathbf{S}$ such that $\boldsymbol{\alpha} = \mathbf{S}\boldsymbol{\beta}$. Firstly we consider the discrepancy between $\boldsymbol{\alpha}$ and $\boldsymbol{\beta}$ to obtain the subscripts t and s:

$$\boldsymbol{\beta} - \boldsymbol{\alpha} = \begin{pmatrix} 10 \\ 10 \\ 5 \\ 2 \\ 1 \end{pmatrix} - \begin{pmatrix} 9 \\ 6 \\ 5 \\ 4 \\ 4 \end{pmatrix} = \begin{pmatrix} 1 \\ 4 \\ 0 \\ -2 \\ -3 \end{pmatrix} \Rightarrow \delta(\boldsymbol{\alpha}, \boldsymbol{\beta}) = 4. \quad (8)$$

We know the discrepancy is the number of nonzero coordinates of the vector $\boldsymbol{\beta} - \boldsymbol{\alpha}$, and t shall be the least subscript of the components such that $\alpha_t > \beta_t$, and s shall be the greatest subscript of the components, less than t, for which $\alpha_s < \beta_s$:

$$\boldsymbol{\alpha} = \begin{pmatrix} \alpha_1 \\ \alpha_2 \\ \alpha_3 \\ \alpha_4 \\ \alpha_5 \end{pmatrix} = (\alpha_i), \quad (9)$$

$$\beta_1 > \alpha_1 \Rightarrow \beta_1 - \alpha_1 > 0, \quad (10)$$

$$\beta_2 > \alpha_2 \Rightarrow \beta_2 - \alpha_2 > 0, \quad (11)$$

$$\beta_3 = \alpha_3 \Rightarrow \beta_3 - \alpha_3 = 0, \quad (12)$$

$$\beta_4 < \alpha_4 \Rightarrow \beta_4 - \alpha_4 < 0, \quad (13)$$

$$\beta_5 < \alpha_5 \Rightarrow \beta_5 - \alpha_5 < 0. \quad (14)$$

From (11) and (13) follows $t = 4$ and $s = 2$.

"Let $\mathbf{S}_1$ be the elementary doubly stochastic $n \times n$ matrix with Θ in position (s,s) and (t,t), and $1-\Theta$ in positions (s,t) and (t,s). Then

$$(\mathbf{S}_1\boldsymbol{\beta})_s = \Theta\beta_s + (1-\Theta)\beta_t, \quad (15)$$

$$(\mathbf{S}_1\boldsymbol{\beta})_t = (1-\Theta)\beta_s + \Theta\beta_t, \quad (16)$$

and

$$(\mathbf{S}_1\boldsymbol{\beta})_i = \beta_i \quad (17)$$

for all other i. We choose two values for Θ:

$$\Theta_1 = \frac{\alpha_s - \beta_t}{\beta_s - \beta_t}, \quad (18)$$

$$\Theta_2 = \frac{\beta_s - \alpha_t}{\beta_s - \beta_t}. \quad (19)$$

Since $\beta_s > \alpha_s \geq \alpha_t > \beta_t$, both these values lie in the interval $(0,1)$. If $\Theta = \Theta_1$, then

$$(\mathbf{S}_1\boldsymbol{\beta})_s = \alpha_s \quad \text{and} \quad (\mathbf{S}_1\boldsymbol{\beta})_t = \beta_s - \alpha_s + \beta_t; \quad (20)$$

and if $\Theta = \Theta_2$, then

$$(\mathbf{S}_1\boldsymbol{\beta})_s = \beta_s - \alpha_t + \beta_t \quad \text{and} \quad (\mathbf{S}_1\boldsymbol{\beta})_t = \alpha_t. \quad (21)$$

Thus in either case the discrepancy between $\boldsymbol{\alpha}$ and $\mathbf{S}_1\boldsymbol{\beta}$ is less than $\delta(\boldsymbol{\alpha}, \boldsymbol{\beta})$, provided that $\boldsymbol{\alpha} \prec \mathbf{S}_1\boldsymbol{\beta}$. This will be the case for Θ_1 if

$$\beta_{t-1} \geq \beta_s - \alpha_s + \beta_t \geq \beta_{t+1}, \quad (22)$$

and for Θ_2 if

$$\beta_{s-1} \geq \beta_s - \alpha_t + \beta_t \geq \beta_{s+1}." \quad (23)$$

Let

$$\mathbf{S}_1 = \begin{pmatrix} 1 & 0 & 0 & 0 & 0 \\ 0 & \Theta & 0 & 1-\Theta & 0 \\ 0 & 0 & 1 & 0 & 0 \\ 0 & 1-\Theta & 0 & \Theta & 0 \\ 0 & 0 & 0 & 0 & 1 \end{pmatrix}. \quad (24)$$

If we take $\Theta = \Theta_1 = (\alpha_2 - \beta_4)/(\beta_2 - \beta_4) = \frac{1}{2}$, then $(\mathbf{S}_1\boldsymbol{\beta})_2 = (\mathbf{S}_1\boldsymbol{\beta})_4 = 6$, and $\mathbf{S}_1\boldsymbol{\beta} = (10\ 6\ 5\ 6\ 1)$. Thus $\mathbf{S}_1\boldsymbol{\beta}^* = (10\ 6\ 6\ 5\ 1)$, and $\delta(\boldsymbol{\alpha}, \mathbf{S}_1\boldsymbol{\beta}) = 4$. We try $\Theta = \Theta_2 = (\beta_2 - \alpha_4)/(\beta_2 - \beta_4) = \frac{3}{4}$. Then $(\mathbf{S}_1\boldsymbol{\beta})_4 = \alpha_4 = 4$, and $\mathbf{S}_1\boldsymbol{\beta} = (10\ 8\ 5\ 4\ 1)$. In this case, $\delta(\boldsymbol{\alpha}, \mathbf{S}_1\boldsymbol{\beta}) = 3 < \delta(\boldsymbol{\alpha}, \boldsymbol{\beta})$.

"[$\cdots$]. Continuing in the same fashion, we can find a sequence of doubly stochastic matrices $\mathbf{S}_1, \mathbf{S}_2, \cdots, \mathbf{S}_k$ such that the discrepancy $\delta(\alpha, \mathbf{S}_k, \mathbf{S}_{k-1} \cdots \mathbf{S}_1 \beta)$ is zero, that is $\alpha = \mathbf{S}_k, \mathbf{S}_{k-1} \cdots \mathbf{S}_1 \boldsymbol{\beta}$. Now set $\mathbf{S} = \mathbf{S}_k, \mathbf{S}_{k-1} \cdots \mathbf{S}_1$, which is doubly stochastic because a product of doubly stochastic matrices is doubly stochastic [4, 5, 8]."

Finally we obtain for this example the doubly stochastic matrix

$$\mathbf{S} = \frac{1}{140} \begin{pmatrix} 112 & 12 & 0 & 4 & 12 \\ 28 & 48 & 0 & 16 & 48 \\ 0 & 0 & 140 & 0 & 0 \\ 0 & 35 & 0 & 105 & 0 \\ 0 & 45 & 0 & 15 & 80 \end{pmatrix}. \qquad (25)$$

With the concept of classical majorization we can define transitions between neighbouring partition diagrams going from the least upper bound to the greatest lower bound.

5. Transitions between Partition Diagrams

All diagrams and state vectors in a Ruch lattice fulfill the conditions of being real nonnegative n-tupels with the same trace, and they satisfy (1), except state vectors ***4a***, ***4b***, and ***6a***, ***6b*** (Fig. 8). If we consider the partial sum vector of the state vectors ***4a*** (***6a***) and ***4b*** (***6b***), we see that no "greater relation" between the vectors is defined in (1), see (26). These states (***4a***, ***4b***, and ***6a***, ***6b***) are called incomparable states.

$$\begin{pmatrix} 3 \\ 6 \\ 6 \\ 6 \\ 6 \\ 6 \end{pmatrix} \begin{matrix} < \\ > \\ = \\ = \\ = \\ = \end{matrix} \begin{pmatrix} 4 \\ 5 \\ 6 \\ 6 \\ 6 \\ 6 \end{pmatrix}, \quad \begin{pmatrix} 2 \\ 4 \\ 6 \\ 6 \\ 6 \\ 6 \end{pmatrix} \begin{matrix} < \\ = \\ > \\ = \\ = \\ = \end{matrix} \begin{pmatrix} 3 \\ 4 \\ 5 \\ 6 \\ 6 \\ 6 \end{pmatrix}. \qquad (26)$$

Equation (26): Comparison of the state vectors ***4a*** and ***6a*** with ***4b*** and ***6b*** through partial sum vectors. ***State 4a*** (***6a***) is neither greater nor less than ***4b*** (***6b***) nor equal to ***4b*** (***6b***). ***4a*** (***6a***) and ***4b*** (***6b***) are incomparable.

Due to the partial order in this lattice (Fig. 8), there are several possibilities starting from the least upper bound (***state 1***) to arrive at the greatest lower bound (***state 9***) along the lines, either via ***4a*** or ***4b*** and either via ***6a*** or ***6b***. But all transitions of the state vectors of one possible path can be described with a doubly stochastic matrix. For instance, a doubly stochastic matrix (27) maps ***state 1*** (600000) on ***state 2*** (510000), another one maps ***state 2*** (510000) on ***state 3*** (420000) (28) and so on.

$$\begin{pmatrix} 5/6 & 1/6 & 0 & 0 & 0 & 0 \\ 1/6 & 5/6 & 0 & 0 & 0 & 0 \\ 0 & 0 & 1 & 0 & 0 & 0 \\ 0 & 0 & 0 & 1 & 0 & 0 \\ 0 & 0 & 0 & 0 & 1 & 0 \\ 0 & 0 & 0 & 0 & 0 & 1 \end{pmatrix} \begin{pmatrix} 6 \\ 0 \\ 0 \\ 0 \\ 0 \\ 0 \end{pmatrix} = \begin{pmatrix} 5 \\ 1 \\ 0 \\ 0 \\ 0 \\ 0 \end{pmatrix}. \qquad (27)$$

Equation (27): $\mathbf{S}_1 \cdot$ (***state 1***) = (***state 2***).

$$\begin{pmatrix} 3/4 & 1/4 & 0 & 0 & 0 & 0 \\ 1/4 & 3/4 & 0 & 0 & 0 & 0 \\ 0 & 0 & 1 & 0 & 0 & 0 \\ 0 & 0 & 0 & 1 & 0 & 0 \\ 0 & 0 & 0 & 0 & 1 & 0 \\ 0 & 0 & 0 & 0 & 0 & 1 \end{pmatrix} \begin{pmatrix} 5 \\ 1 \\ 0 \\ 0 \\ 0 \\ 0 \end{pmatrix} = \begin{pmatrix} 4 \\ 2 \\ 0 \\ 0 \\ 0 \\ 0 \end{pmatrix}. \qquad (28)$$

Equation (28): $\mathbf{S}_2 \cdot$ (***state 2***) = (***state 3***).

The doubly stochastic matrices in (27) and (28) are nonsingular, and therefore are invertible. However, some transitions are characterized by doubly stochastic matrices which are singular and therefore are not invertible [see (29) and (30)]. We see that the doubly stochastic matrix $\mathbf{S}_3$ (29) is singular because the first and second row and column, respectively, are linearly dependent and the determinant of $\mathbf{S}_3$ becomes equal to zero. Only if the determinant is not zero one can compute the inverse of $\mathbf{S}_3$ (31). Thus one may speak of reversible transitions characterized by invertible doubly stochastic matrices, and of irreversible transitions characterized by noninvertible doubly stochastic matrices.

$$\begin{pmatrix} 1/2 & 1/2 & 0 & 0 & 0 & 0 \\ 1/2 & 1/2 & 0 & 0 & 0 & 0 \\ 0 & 0 & 1 & 0 & 0 & 0 \\ 0 & 0 & 0 & 1 & 0 & 0 \\ 0 & 0 & 0 & 0 & 1 & 0 \\ 0 & 0 & 0 & 0 & 0 & 1 \end{pmatrix} \begin{pmatrix} 4 \\ 2 \\ 0 \\ 0 \\ 0 \\ 0 \end{pmatrix} = \begin{pmatrix} 3 \\ 3 \\ 0 \\ 0 \\ 0 \\ 0 \end{pmatrix}. \qquad (29)$$

Equation (29): $\mathbf{S}_3 \cdot$ (***state 3***) = (***state 4a***).

$$\begin{pmatrix} 1 & 0 & 0 & 0 & 0 & 0 \\ 0 & 1/2 & 1/2 & 0 & 0 & 0 \\ 0 & 1/2 & 1/2 & 0 & 0 & 0 \\ 0 & 0 & 0 & 1 & 0 & 0 \\ 0 & 0 & 0 & 0 & 1 & 0 \\ 0 & 0 & 0 & 0 & 0 & 1 \end{pmatrix} \begin{pmatrix} 4 \\ 2 \\ 0 \\ 0 \\ 0 \\ 0 \end{pmatrix} = \begin{pmatrix} 4 \\ 1 \\ 1 \\ 0 \\ 0 \\ 0 \end{pmatrix}. \qquad (30)$$

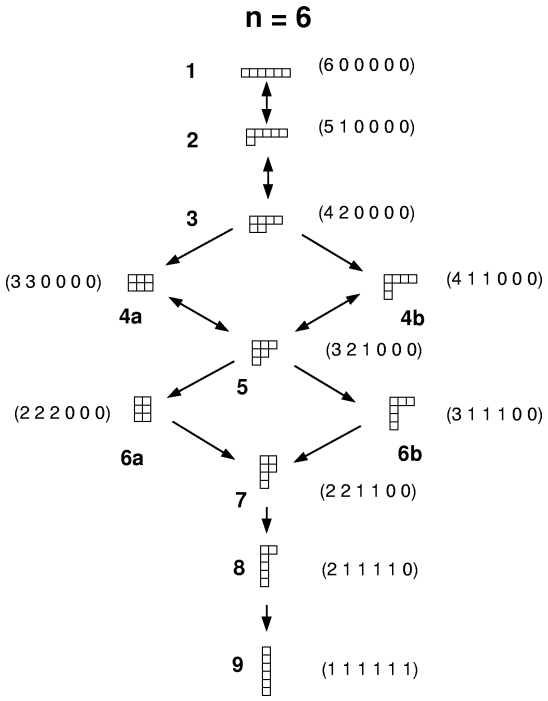

Fig. 10. The $n = 6$ Ruch lattice with all first order transitions (characterized by doubly stochastic matrices). Singular doubly stochastic matrices describe irreversible transitions (arrow), invertible doubly stochastic matrices describe reversible transitions (double-headed arrow).

Equation (30): $\mathbf{S}_4 \cdot$ (***state 3***) = (***state 4b***). 31

$$\mathbf{S}_3^{-1} = \frac{\text{adjugate}\,\mathbf{S}_3}{\text{determinant}\,\mathbf{S}_3}. \tag{31}$$

In Fig. 10 all so-called irreversible transitions are characterized by an arrow, and all so-called reversible transitions are characterized by a double-headed arrow. All these transitions we call first order transitions. That is, first order transitions are transitions between neighbouring states. Near the greatest lower bound all first order transitions are irreversible.

There is also the possibility to have higher order transitions, e. g. from ***state 5*** to ***state 7***, leaving out ***states 6a*** and ***6b***. Higher order transitions are also characterized by either invertible or noninvertible doubly stochastic matrices. All possible transitions for the $n = 6$ lattice are shown in Table 1. It is noteworthy, that the doubly stochastic matrices for higher order transitions are not necessarily the product of doubly stochastic matrices of first order transitions. For instance the second order transition from ***state 5*** to ***state 7*** is characterized by invertible doubly stochastic matrices (36),

Table 1. Reversible (1) and irreversible (0) transitions. The bold numbers stand for first order transitions, see Figure 10.

	1	2	3	4a	4b	5	6a	6b	7	8	9
1	1	**1**	1	0	0	1	0	0	1	1	0
2	1	1	**1**	0	1	1	0	0	1	1	0
3	1	1	1	**0**	**0**	1	0	0	1	0	0
4a	0	0	0	1	0	**1**	0	0	1	0	0
4b	0	1	0	0	1	**1**	0	1	1	1	0
5	1	1	1	1	1	1	**0**	**0**	1	0	0
6a	0	0	0	0	0	0	1	0	**0**	0	0
6b	0	0	0	0	1	0	0	1	**0**	1	0
7	1	1	1	1	1	1	0	0	1	**0**	0
8	1	1	0	0	1	0	0	1	0	1	**0**
9	0	0	0	0	0	0	0	0	0	0	1

but the transitions from ***state 5*** to ***state 6a*** (32) and from ***state 6a*** to ***state 7*** (33) are characterized by noninvertible doubly stochastic matrices, and the product of these first order doubly stochastic matrices (34) is also not invertible [see (35)].

$$\begin{pmatrix} 1/2 & 0 & 1/2 & 0 & 0 & 0 \\ 0 & 1 & 0 & 0 & 0 & 0 \\ 1/2 & 0 & 1/2 & 0 & 0 & 0 \\ 0 & 0 & 0 & 1 & 0 & 0 \\ 0 & 0 & 0 & 0 & 1 & 0 \\ 0 & 0 & 0 & 0 & 0 & 1 \end{pmatrix} \begin{pmatrix} 3 \\ 2 \\ 1 \\ 0 \\ 0 \\ 0 \end{pmatrix} = \begin{pmatrix} 2 \\ 2 \\ 2 \\ 0 \\ 0 \\ 0 \end{pmatrix}. \tag{32}$$

Equation (32): $\mathbf{S}_5 \cdot$ (***state 5***) = (***state 6a***): Irreversible first order transition.

$$\begin{pmatrix} 1 & 0 & 0 & 0 & 0 & 0 \\ 0 & 1 & 0 & 0 & 0 & 0 \\ 0 & 0 & 1/2 & 1/2 & 0 & 0 \\ 0 & 0 & 1/2 & 1/2 & 0 & 0 \\ 0 & 0 & 0 & 0 & 1 & 0 \\ 0 & 0 & 0 & 0 & 0 & 1 \end{pmatrix} \begin{pmatrix} 2 \\ 2 \\ 2 \\ 0 \\ 0 \\ 0 \end{pmatrix} = \begin{pmatrix} 2 \\ 2 \\ 1 \\ 1 \\ 0 \\ 0 \end{pmatrix}. \tag{33}$$

Equation (33): $\mathbf{S}_6 \cdot$ (***state 6a***) = (***state 7***): Irreversible first order transition.

$$\begin{pmatrix} 1 & 0 & 0 & 0 & 0 & 0 \\ 0 & 1 & 0 & 0 & 0 & 0 \\ 0 & 0 & 1/2 & 1/2 & 0 & 0 \\ 0 & 0 & 1/2 & 1/2 & 0 & 0 \\ 0 & 0 & 0 & 0 & 1 & 0 \\ 0 & 0 & 0 & 0 & 0 & 1 \end{pmatrix}$$

$$\cdot \begin{pmatrix} 1/2 & 0 & 1/2 & 0 & 0 & 0 \\ 0 & 1 & 0 & 0 & 0 & 0 \\ 1/2 & 0 & 1/2 & 0 & 0 & 0 \\ 0 & 0 & 0 & 1 & 0 & 0 \\ 0 & 0 & 0 & 0 & 1 & 0 \\ 0 & 0 & 0 & 0 & 0 & 1 \end{pmatrix} \begin{pmatrix} 3 \\ 2 \\ 1 \\ 0 \\ 0 \\ 0 \end{pmatrix} = \begin{pmatrix} 2 \\ 2 \\ 1 \\ 1 \\ 0 \\ 0 \end{pmatrix}. \tag{34}$$

Equation (34): $\mathbf{S}_6 S_5 \cdot$ (***state 5***) = (***state 7***): Product of irreversible first order transitions.

$$\begin{pmatrix} 1/2 & 0 & 1/2 & 0 & 0 & 0 \\ 0 & 1 & 0 & 0 & 0 & 0 \\ 1/4 & 0 & 1/4 & 1/2 & 0 & 0 \\ 1/4 & 0 & 1/4 & 1/2 & 0 & 0 \\ 0 & 0 & 0 & 0 & 1 & 0 \\ 0 & 0 & 0 & 0 & 0 & 1 \end{pmatrix} \begin{pmatrix} 3 \\ 2 \\ 1 \\ 0 \\ 0 \\ 0 \end{pmatrix} = \begin{pmatrix} 2 \\ 2 \\ 1 \\ 1 \\ 0 \\ 0 \end{pmatrix}. \quad (35)$$

Equation (35): $\mathbf{S}_7 \cdot$ (***state 5***) = (***state 7***): Irreversible second order transition.

$$\begin{pmatrix} 2/3 & 0 & 0 & 1/3 & 0 & 0 \\ 0 & 1 & 0 & 0 & 0 & 0 \\ 0 & 0 & 1 & 0 & 0 & 0 \\ 1/3 & 0 & 0 & 2/3 & 0 & 0 \\ 0 & 0 & 0 & 0 & 1 & 0 \\ 0 & 0 & 0 & 0 & 0 & 1 \end{pmatrix} \begin{pmatrix} 3 \\ 2 \\ 1 \\ 0 \\ 0 \\ 0 \end{pmatrix} = \begin{pmatrix} 2 \\ 2 \\ 1 \\ 1 \\ 0 \\ 0 \end{pmatrix}. \quad (36)$$

Equation (36): $\mathbf{S}_8 \cdot$ (***state 5***) = (***state 7***): Reversible second order transition.

The transitions between incomparable states only can be described by the product of a doubly stochastic matrix with an inverse of another doubly stochastic matrix, if this inverse matrix exists. The product of a doubly stochastic matrix with the inverse of a doubly stochastic matrix will be called pseudo doubly stochastic matrix $\mathbf{S}_p$. In the following we will see, how to generate the pseudo doubly stochastic matrix $\mathbf{S}_p$ for the transition from ***state 4a*** to ***state 4b***. We do this in the same manner as described in Section 4.

We compute the discrepancy (8) of the state vectors ***4a*** and ***4b*** and the subscripts t and s [(9)−(14)] to obtain the components of the pseudo doubly stochastic matrix $\mathbf{S}_p$ (18) and (19): $\delta(\mathbf{4a}, \mathbf{4b}) = 3$ and $s = 2$, $t = 3$, $[4, 5, 8]$, see (37) and (38).

$$\begin{pmatrix} 3 \\ 3 \\ 0 \\ 0 \\ 0 \\ 0 \end{pmatrix} - \begin{pmatrix} 4 \\ 1 \\ 1 \\ 0 \\ 0 \\ 0 \end{pmatrix} = \begin{pmatrix} -1 \\ 2 \\ -1 \\ 0 \\ 0 \\ 0 \end{pmatrix}. \quad (37)$$

$$\begin{pmatrix} 1 & 0 & 0 & 0 & 0 & 0 \\ 0 & 2/3 & 1/3 & 0 & 0 & 0 \\ 0 & 1/3 & 2/3 & 0 & 0 & 0 \\ 0 & 0 & 0 & 1 & 0 & 0 \\ 0 & 0 & 0 & 0 & 1 & 0 \\ 0 & 0 & 0 & 0 & 0 & 1 \end{pmatrix} \begin{pmatrix} 3 \\ 3 \\ 0 \\ 0 \\ 0 \\ 0 \end{pmatrix} = \begin{pmatrix} 3 \\ 2 \\ 1 \\ 0 \\ 0 \\ 0 \end{pmatrix}. \quad (38)$$

Equation (38): $\mathbf{S}_9 \cdot$ (***state 4a***) = ***state***($\mathbf{S}_9 \cdot$ (***state 4a***)).

Now we consider the partial sum vectors of ***state***($\mathbf{S}_9 \cdot$ (***state 4a***)) and ***state 4b***, and we see that ***state***($\mathbf{S}_9 \cdot$ (***state 4a***)) $\prec$ ***state 4b***, compare Definition 1 in Section 4. Next we try to find a matrix $\mathbf{S}_{10}$ satisfying $\mathbf{S}_{10} \cdot$ (***state 4b***) = $\mathbf{S}_9 \cdot$ (***state 4a***).

$$\begin{pmatrix} 2/3 & 1/3 & 0 & 0 & 0 & 0 \\ 1/3 & 2/3 & 0 & 0 & 0 & 0 \\ 0 & 0 & 1 & 0 & 0 & 0 \\ 0 & 0 & 0 & 1 & 0 & 0 \\ 0 & 0 & 0 & 0 & 1 & 0 \\ 0 & 0 & 0 & 0 & 0 & 1 \end{pmatrix} \begin{pmatrix} 4 \\ 1 \\ 1 \\ 0 \\ 0 \\ 0 \end{pmatrix} = \begin{pmatrix} 3 \\ 2 \\ 1 \\ 0 \\ 0 \\ 0 \end{pmatrix}. \quad (39)$$

Equation (39): $\mathbf{S}_{10} \cdot$ (***state 4b***) = ***state***($\mathbf{S}_{10} \cdot$ (***state 4b***)) = ***state***($\mathbf{S}_9 \cdot$ (***state 4a***)).

It is easy to see that ***state***($\mathbf{S}_9 \cdot$ (***state 4a***)) and ***state***($\mathbf{S}_{10} \cdot$ (***state 4b***)) describe ***state 5***. Now we can arrive at ***state 4b*** from ***state 4a*** and vice versa via ***state 5***, see (40) and (41). In this case the matrices describe second order transitions.

$$\begin{pmatrix} 2 & -2/3 & -1/3 & 0 & 0 & 0 \\ -1 & 4/3 & 2/3 & 0 & 0 & 0 \\ 0 & 1/3 & 2/3 & 0 & 0 & 0 \\ 0 & 0 & 0 & 1 & 0 & 0 \\ 0 & 0 & 0 & 0 & 1 & 0 \\ 0 & 0 & 0 & 0 & 0 & 1 \end{pmatrix} \begin{pmatrix} 3 \\ 3 \\ 0 \\ 0 \\ 0 \\ 0 \end{pmatrix} = \begin{pmatrix} 4 \\ 1 \\ 1 \\ 0 \\ 0 \\ 0 \end{pmatrix}. \quad (40)$$

Equation (40): $\mathbf{S}_{10}^{-1} \mathbf{S}_9 \cdot$ (***state 4a***) = $\mathbf{S}_{p_1} \cdot$ (***state 4a***) = ***state 4b***.

$$\begin{pmatrix} 2/3 & 1/3 & 0 & 0 & 0 & 0 \\ 2/3 & 4/3 & -1 & 0 & 0 & 0 \\ -1/3 & -2/3 & 2 & 0 & 0 & 0 \\ 0 & 0 & 0 & 1 & 0 & 0 \\ 0 & 0 & 0 & 0 & 1 & 0 \\ 0 & 0 & 0 & 0 & 0 & 1 \end{pmatrix} \begin{pmatrix} 4 \\ 1 \\ 1 \\ 0 \\ 0 \\ 0 \end{pmatrix} = \begin{pmatrix} 3 \\ 3 \\ 0 \\ 0 \\ 0 \\ 0 \end{pmatrix}. \quad (41)$$

Equation (41): $\mathbf{S}_9^{-1} \mathbf{S}_{10} \cdot$ (***state 4b***) = $\mathbf{S}_{p_2} \cdot$ (***state 4b***) = ***state 4a***.

The row and column sums of the pseudo doubly stochastic matrices $\mathbf{S}_{p_1}$ and $\mathbf{S}_{p_2}$ [(40) and (41)] are one, but now we have positive *and* negative elements in the pseudo doubly stochastic matrix.

If we consider the ***states 6a*** and ***6b***, only higher order transitions between these states are possible. For example, one possible path from ***state 6a*** to ***state 6b*** goes via ***state 7*** to ***state 5***, see (42):

$$\begin{aligned} \textbf{\textit{state 6a}} \xrightarrow{a} \textbf{\textit{state 7}} \xrightarrow{b} \textbf{\textit{state 5}} \xrightarrow{c} \textbf{\textit{state 6b}} \\ \Rightarrow \textbf{\textit{state 6a}} \xrightarrow{d} \textbf{\textit{state 6b}}, \end{aligned} \quad (42)$$

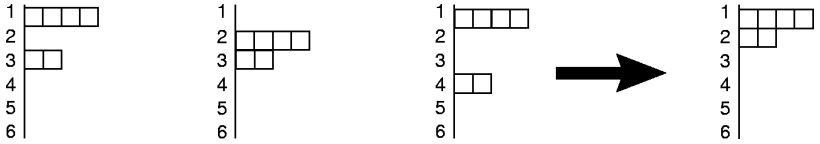

Fig. 11. Some mixing-equivalent permutations of the state $(4\,2\,0\,0\,0\,0)$.

where a is a irreversible first order transition, b a reversible second order transition, c a irreversible first order transition, d a irreversible fourth order transition. Note that higher order transitions may be direct transitions or may be comprised of lower order transitions, compare (32) – (36).

In Table 1 one sees that, except of ***state 9***, transitions between all other states are possible. ***State 9*** ("the equilibrium state") defines a point of no return.

Since our foam system is an open system which shows structure formation [1] during the foam decay process, we extended by the introduction of reversible transitions the Ruch modell, which originally considered irreversible processes in closed systems [2]. That means, transitions with entropy loss become possible.

6. Sets of Mixing-Equivalent States

Now let a partition diagram be not only one state but also a representative for all permutations of this state, see Figure 11. The transitions between states and their permutations do not change by multiplying the doubly stochastic matrices by permutation matrices (see also theorems of Muirhead [4] and of Hardy, Littlewood and Pólya [5]). You may also say, that the Shannon entropy or the mixing character does not change [2].

The order or respectively the partial order of the partition diagrams in a Ruch lattice (Fig. 8) is derived by the componentwise comparison of the partial sum vectors of the state vectors. Note that the state vectors are not rearranged in any order. With the same method we can generate a permutation lattice of a state. We permute the state $(4\,2\,0\,0\,0\,0)$ without changing the order of the nonzero elements. By comparing the partial sum vectors we obtain the permutation lattice of the state $(4\,2\,0\,0\,0\,0)$, see Figure 12. An isomorphic lattice exists for the state $(2\,4\,0\,0\,0\,0)$, which is a permutation of the nonzero elements of the state $(4\,2\,0\,0\,0\,0)$. The number of all permutations P of the state $(4\,2\,0\,0\,0\,0)$ is given by

$$P_{n,n_1,n_2,\cdots} = \frac{n!}{n_1!\,n_2!\,n_3!\cdots} \Rightarrow \frac{6!}{1!\,1!\,4!} = 30, \quad (43)$$

Table 2. Each state s of the $n = 6$ Ruch lattice has a specific number of permutations $P(s)$ which is given by (43).

s	1	2	3	4a	4b	5	6a	6b	7	8	9	Σ 11
$P(s)$	6	30	30	15	60	120	20	60	90	30	1	Σ **462**

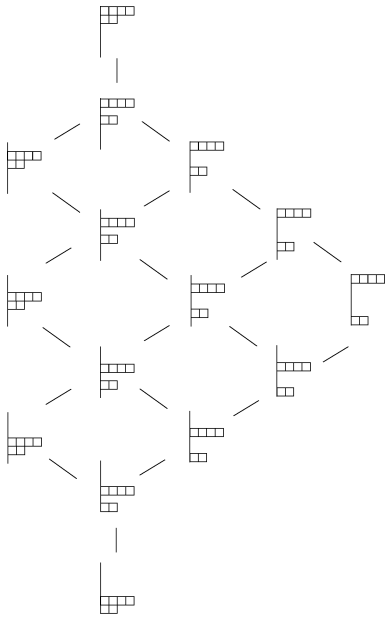

Fig. 12. Permutation lattice of the state (420000) computed via partial sums. An isomorphic lattice exists for the state (240000), which one obtains by permuting the nonzero elements of the state (420000).

whereas the number of factors n_i in the denominator is given by the number of sets of equal elements.

Table 2 shows the number of all permutations $P(s)$ of the states s in the 6 cell Ruch lattice.

Table 3 shows the number of partitions $p(n)$ and the sums of all permutations $P(n)$, (44), of the $n = 1$ Ruch lattice up to $n = 9$:

$$\sum_{i=1}^{k} P(s_i) = P(n), \quad i = 1,2,\cdots,k, \quad k = p(n). \quad (44)$$

The union of both lattices of the states (420000) and (240000) is not a lattice, but a partially ordered set (poset). In Fig. 13 we see the upper part of the

Table 3. The number of partitions $p(n)$ [6] of $n = 1$ up to $n = 9$ Ruch lattice. $P(n)$ describes the sums of the permutations $P(s)$, (44), of a Ruch lattice. One can find $P(6)$ (bold number) in Table 2 (bold number).

n	1	2	3	4	5	6	7	8	9
$p(n)$	1	2	3	5	7	11	15	22	30
$P(n)$	1	3	10	35	126	**462**	1716	6435	24310

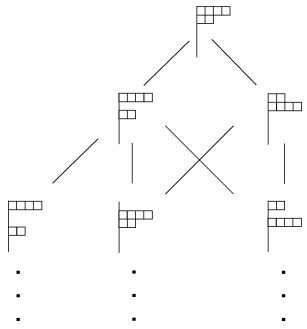

Fig. 13. Upper part of the poset obtained from the union of the isomorphic permutation lattices of the states (420000) and (240000). The poset is derived by the componentwise comparison of the partial sum vectors of these states.

united isomorphic permutation lattices of the states (420000) and (240000).

We extended the concept of Ruch lattices through the introduction of permutations of partition diagrams. If we construct the union of the permutation lattices, the lattice character is lost and we obtain a partially orderd set (poset). We did this to enable the characterization of experimental bubble size distributions.

7. Bubble Size Distribution Functions

We have seen that partially ordered Ruch lattices provide many opportunities. We like to take on this theoretical approach and apply it to our bubble size distributions. However, at first we consider the procedure of foam measurement. For example one pours 20 ml of beer in a rectangular glass vessel ($2.5 \cdot 2.5$ cm) at (24 ± 1) °C (this "unfoamed beer" is allowed only to posses at most 5% of foam with respect to its fluid part) and froths up the beer with ultrasound (Ultrasonik 28×; NEY) for 13 s until there is no more foam development. In order to estimate the bubble size distribution function, we have taken photographs with a CCD-camera (JAI CV-A11; lens 1 : 0; resolution 72 pixel/cm or 300 pixel/cm). 30 s after frothing up, we took pictures every 25 s.

In Fig. 14 we see the temporal development (30 s, 60 s, 260 s) of the bubble size distribution. To compare the bubble size distributions with different numbers of bubbles, each bubble size distribution is normed to unity. At the beginning we see a very narrow distribution because of the ultrasound treatment of the beer sample. After 60 s, we observe a broadening of the distribution function, as can be expected from an ordinary diffusion. At the end, after 260 s, we obtain a multimodal distribution with small full widths at half maximum. Only very few and quite different bubble sizes survived [1].

Bubble size distributions can be represented as vectors (state vectors). In our case we obtain state vectors with 10 components. The components of the vectors are the number of bubbles belonging to a certain bubble size interval. As the distributions are normed to unity, all state vectors have the same trace (to obtain integer components and state vectors with the same trace we can compute the least common multiple of all original state vector traces). These state vectors can be rearranged in nonincreasing order, and we obtain bubble size distributions in which bubble size intervals are rearranged in nonincreasing relative frequency (the order is given by the normed diameter d^*) as is shown in Figure 15.

We will compare all bubble size distributions with each other. So we take the rearranged state vectors of the bubble size distributions and consider the partial sums of these state vectors. In Table 4 one sees which states [abbreviated s (time in seconds)] are majorized ($\prec$) by others and which states are incomparable ($\sim$).

It is easy to note in Table 4 that the overlined states describe the temporal development of the state vectors and the mixing character increases and decreases: $s_0 \succ s_1 \succ s_2$ (mixing character increases), $s_2 \sim s_3 \sim s_4$ (marginal change of the mixing character), $s_4 \prec s_5$ (mixing character decreases), and so on. We will say the mixing character oscillates. To show this behaviour, we map the bubble size distributions on the Shannon entropy [1, 2, 9], see (45):

$$I(\gamma) = -\sum_{i=1}^{n} v_i \; ld \; v_i. \tag{45}$$

In chronological order the Shannon entropy of the bubble size distributions shows an oscillating behaviour, (see Fig. 16). This oscillating behaviour characterizes the phase of rearrangement [1] within the foam.

Since we do not have an equal distribution at the end of the rearrangement in the foam decay process, and

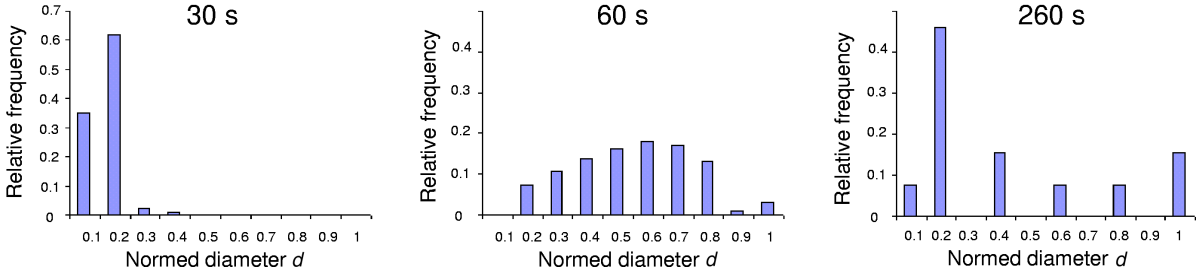

Fig. 14. The temporal development of the bubble size distribution after 30 s, 60 s and 260 s. Each distribution is normed to unity to make the distributions comparable. These bubble size distributions are permutations of the bubble size distributions in Figure 15. In Fig. 15 the bubble size intervals are rearranged in nonincreasing relative frequency.

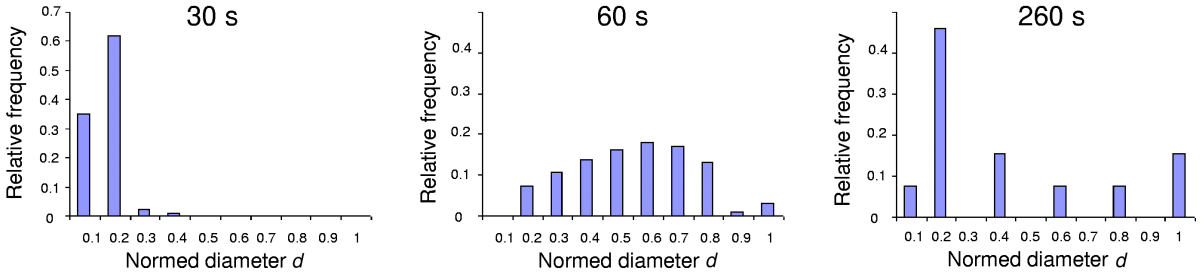

Fig. 15. The temporal development of the bubble size distribution after 30 s, 60 s, and 260 s. All distributions are normed to unity and the bubble size intervals are rearranged in nonincreasing relative frequency (the order is given by the normed diameter d^*). In Fig. 14 we see corresponding permutations of these "rearranged" distributions.

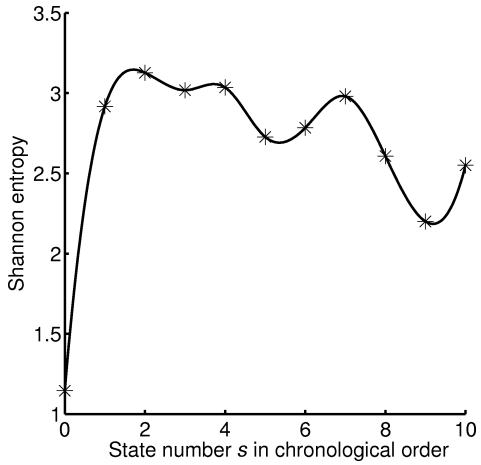

Fig. 16. The Shannon entropy and mixing character, respectively, of the bubble size distributions approximately oscillate.

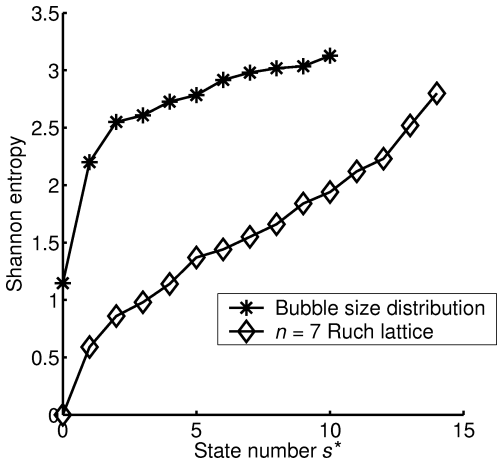

Fig. 17. The states of the bubble size distributions and the partition diagrams of the $n = 7$ Ruch lattice rearranged in increasing Shannon entropy.

we only measured bubble size distributions every 25 s, not all possible distributions are known. Therefore we cannot construct a complete Ruch lattice. But we find a similar behaviour: In Table 4, at the beginning of the foam decay, we see ordered states. Later, the states become partially ordered and therefore incomparable. Figure 17 shows the states of the bubble size distributions and the partition diagrams of the $n = 7$ Ruch lattice rearranged in increasing Shannon entropy. The last four partition diagrams of the $n = 7$ Ruch lattice are partition diagrams which are comparable to distributions lying near the equal distribution.

If we rearrange the states s_i of the bubble size distribution in ascending Shannon entropy I, and calculate

s_0 30 s	s_1 60s	s_2 85 s	s_3 110 s	s_4 135 s	s_5 160 s	s_6 185 s	s_7 210 s	s_8 235 s	s_9 260 s	s_{10} 285 s
$\succ \overline{s_1}$										
$\succ s_2$	$\succ \overline{s_2}$									
$\succ s_3$	$\sim s_3$	$\sim \overline{s_3}$								
$\succ s_4$	$\sim s_4$	$\sim s_4$	$\sim \overline{s_4}$							
$\succ s_5$	$\prec s_5$	$\prec s_5$	$\prec \mathbf{s_5}$	$\prec \overline{s_5}$						
$\succ s_6$	$\sim s_6$	$\sim s_6$	$\sim s_6$	$\sim s_6$	$\sim \overline{s_6}$					
$\succ s_7$	$\sim s_7$	$\sim s_7$	$\sim s_7$	$\sim s_7$	$\sim s_7$	$\succ \overline{s_7}$				
$\succ s_8$	$\prec s_8$	$\prec s_8$	$\prec s_8$	$\prec s_8$	$\sim s_8$	$\sim s_8$	$\prec \overline{s_8}$			
$\succ s_9$	$\prec s_9$	$\prec s_9$	$\prec s_9$	$\prec s_9$	$\prec s_9$	$\prec s_9$	$\prec s_9$	$\prec \overline{s_9}$		
$\succ \mathbf{s_{10}}$	$\prec s_{10}$	$\prec s_{10}$	$\prec s_{10}$	$\prec s_{10}$	$\prec s_{10}$	$\sim s_{10}$	$\prec s_{10}$	$\prec s_{10}$	$\succ \overline{s_{10}}$	

Table 4. Majorization and incomparableness of the state vectors. For example, we see in the second column state s_1 after 60 s is incomparable ($\sim$) to state s_4 (fourth row) and is majorized by state s_5 (fifth row). All transitions are reversible, except the bold ones. The overlined states describe the temporal development of the state vectors.

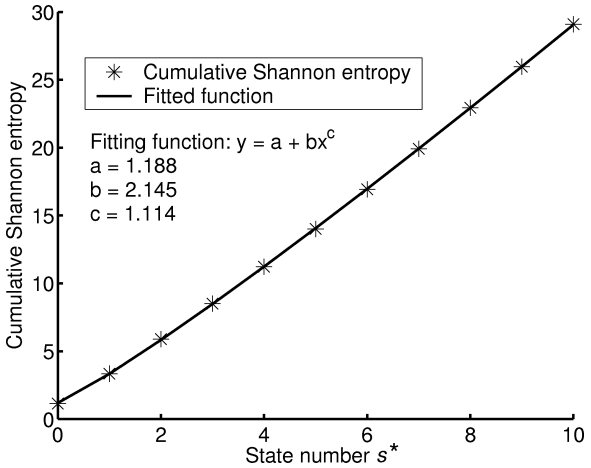

Fig. 18. The partial sums of the increasing Shannon entropy of the bubble size distributions against the states rearranged in increasing Shannon entropy. The power law fitting function has $R^2 = 0.9999$.

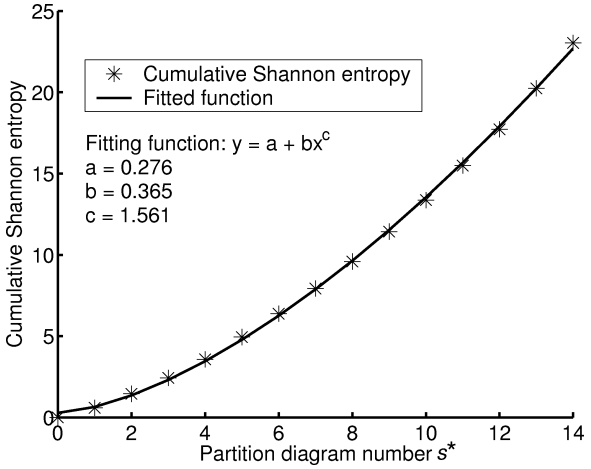

Fig. 19. The increasing Shannon entropy defines the order of the partition diagrams for the $n = 7$ Ruch lattice. Here we see the partition diagram order as a function of the cumulative Shannon entropy of the partition diagrams. The power law fitting function has $R^2 = 0.9995$.

the partial sums $\sum_{i=0}^{k} I(s_i^*)$ with $k = 1, \cdots, 10$ (cumulative Shannon entropy), we obtain a power law function: $\sum_{i=0}^{k} I(s_i^*) = a + b\,(s_i^*)^c$, with $k = 1, \cdots, 10$, $a = 1.188$, $b = 2.145$, and $c = 1.114$, $R^2 = 0.9999$, shown in Figure 18.

The cumulative Shannon entropy $\sum_{i=0}^{k} I(s_i^*)$ ($k = 1, \cdots, 14$) of the partition diagrams s_i for the $n = 7$ Ruch lattice is plotted against the order of the partition diagrams s_i^* defined by the increasing Shannon entropy, see Figure 19. Again we obtain a power law function: $\sum_{i=0}^{k} I(s_i^*) = a + b\,(s_i^*)^c$, with $k = 1, \cdots, 14$, $a = 0.276$, $b = 0.365$, and $c = 1.561$, $R^2 = 0.9995$. Note that in this case we counted the number of the partition diagrams from $i = 0$ to $p(n) - 1$, to make this function comparable to the function of the bubble size states shown in Figure 18. We infer that both systems are comparable because of the similar behaviour of the cumulative Shannon entropy.

8. Summary and Conclusion

We have seen that the bubble size distributions during foam decay do not follow the development of an ordinary diffusion process. This means that our very narrow bubble size distribution does not end in a more or less equal distribution, but in a distinct multimodal distribution at the end of the rearrangement phase [1, 7]. Furthermore, the temporal development of certain bubble size intervals behaves in-phase or out-of-phase. The partition diagrams of an n-cell Ruch lattice can be represented by vectors, which have trace and dimension n [1, 2]. By permuting these vectors, the number of possible partition diagrams increases extremely (for instance: the 11 vectors representing an $n = 6$ Ruch lattice have 462 permutations). For every permutation of nonzero vector components we obtain permutation lattices which, when being united, lead to posets (we change the propositional calculus). Additionally, transitions are possible between all vec-

tors (of a Ruch lattice) and their permutations. These transitions are defined by doubly stochastic matrices, their inverses, permutation matrices, and pseudo doubly stochastic matrices, unless one arrives at the greatest lower bound, which characterizes the equal distribution (the point of no return). All transitions are either reversible or irreversible, depending on the invertibility of the resulting matrix. With the introduction of reversible transitions we are able to describe structure formation in an open system, which usually is accompanied by a decrease of the entropy of the system. Based on the Ruch lattices we found that we can compare distributions like bubble size distributions. The comparability refers to the statistical order and statistical disorder, respectively. The transition from one distribution $\boldsymbol{\beta}$ to another one $\boldsymbol{\alpha}$ can be characterized by saying: the mixing character increases; the Shannon entropy increases; $\boldsymbol{\alpha}$ is majorized by $\boldsymbol{\beta}$ ($\boldsymbol{\alpha} \prec \boldsymbol{\beta}$); there is a doubly stochastic matrix $\mathbf{S}$ satisfying $\mathbf{S}\boldsymbol{\beta} = \boldsymbol{\alpha}$, or the statistical order decreases and the statistical disorder increases respectively [2 – 5, 9]. But there is yet another characterization. Two distributions $\boldsymbol{\beta}'$ and $\boldsymbol{\alpha}'$ can be incomparable. That means: There is only a marginal change of the mixing character and the Shannon entropy respectively; $\boldsymbol{\alpha}'$ is not majorized by $\boldsymbol{\beta}'$ and vice versa; there is no doubly stochastic matrix $\mathbf{S}$, but a pseudo doubly stochastic matrix $\mathbf{S}_p$ satisfying $\mathbf{S}_p\boldsymbol{\beta}' = \boldsymbol{\alpha}'$, or the statistical order (disorder) changes only marginally, but the distributions can be different. Additionally, we can characterize the transitions by considering the corresponding matrices (doubly stochastic or pseudo doubly stochastic). If the determinant of a transition matrix is not zero, then there exists an inverse to this matrix and we call such a transition reversible. We have noticed in Table 4 that only two transitions of the bubble size distributions are irreversible. In Fig. 16 it is shown that the Shannon entropy oscillates. This behaviour describes the rearrangement in the foam, like bursting, merging, changing size by gas exchange and movement of the bubbles. If we rearrange the bubble size distributions and the partition diagrams of the $n = 7$ Ruch lattice in increasing Shannon entropy (Fig. 17), we see a similar functional behaviour [compare the partial sums of the increasing Shannon entropy of the $n = 7$ Ruch lattice and the bubble size distributions (Fig. 18 and Fig. 19)]. This does not mean that the $n = 7$ Ruch lattice exactly characterizes the bubble size distributions, but possibly parts of Ruch lattices of higher n might describe these bubble size distributions more precisely.

Taking into account the decrease of the number of bubbles during the foam decay process, one may consider transitions from higher number n Ruch lattices to smaller ones. That means, considering that a Ruch lattice may represent a diffusion process with incomparable states, the general progression of the vertical diffusion process inside one Ruch lattice is interrupted by a transition to a smaller Ruch lattice in which the process continues and will be interrupted again by a transition to an even smaller Ruch lattice. The overall process of transitions to Ruch lattices of decreasing order describes the overall decrease in the number of the bubbles and might be responsible for the oscillating behaviour of the Shannon entropy.

We are convinced that our extended Ruch concept combined with classical majorization provides promising features, which enable us to describe not only irreversible processes in closed systems but also more general processes in open systems, like structure formation.

Acknowledgement

We are indebted to E. C. Haß for inspiring discussions.

[1] S. Sauerbrei, E. C. Haß, and P. J. Plath, Discrete Dynamics in Nature and Society (accepted).
[2] E. Ruch, Theor. Chim. Acta **38**, 167 (1975).
[3] P. M. Alberti and A. Uhlmann, Dissipative Motion in State Spaces, Teubner Texte zur Mathematik, Bd. 33, Teubner, Leipzig 1981.
[4] R. F. Muirhead, Proc. Edinburgh Math. Soc. **21**, 144 (1903).
[5] G. H. Hardy, J. E. Littlewood, and G. Pólya, Inequalities, Cambridge University Press, London 1934.
[6] H. Rademacher, Proc. London Math. Soc. **43**, 241 (1937).
[7] M. Potreck, Optimierte Messung der Bierschaumstabilität in Abhängigkeit von Milieubedingungen und fluiddynamischen Kennwerten, Dissertation, TU Berlin 2004, p. 30.
[8] H. Minc, Nonnegative Matrices, John Wiley & Sons Inc., New York 1988, pp. 105 – 117.
[9] C. E. Shannon, A Mathematical Theory of Communication, The Bell System Technical Journal **27**, 379, 623 (1948).